

Study on tank shape for sloshing assessment of LNG vessels under unrestricted filling operation

Jong-Jin Park¹ · Sang-Yeob Kim² · Yonghwan Kim² · Jang-Hoon Seo¹ · Chang-Hun Jin¹ · Ki-Hun Joh¹ · Byung-Woo Kim¹ · Yong-Suk Suh¹

Received: 13 October 2014 / Accepted: 1 May 2015 / Published online: 16 May 2015
© JASNAOE 2015

Abstract Conventional liquefied natural gas (LNG) vessels with membrane cargo containment systems have tank filling restrictions from 0.10 to 0.70 H (with H the internal tank height). The main reason for such restrictions is high sloshing loads around these filling depths. The new designs of prismatic LNG cargo tanks are proposed by increasing the lower chamfer length. Numerical sloshing analysis was used to optimize tank shape out of the several candidates. To validate the effectiveness of the modified tank, 1/50 scaled model tests were conducted. In these tests, 24 different irregular seaways were tested for both the conventional and the optimized tank and their statistical pressures were compared. Modified tank design was quite effective in reducing sloshing loads for a 0.30 H filling depth, and it did not significantly increase sloshing loads at other filling conditions. This study demonstrated the possibility of all filling operations for an LNG cargo containment system.

Keywords Sloshing · LNG vessel · Tank optimization · LNG cargo containment system

1 Introduction

Liquefied natural gas (LNG) carriers with a membrane cargo containment system generally have tank filling restrictions between 0.10 and 0.70 H (with H the

internal tank height). The main reason for filling depth restrictions is the high sloshing pressures around 0.20 to 0.40 H tank filling depths [1–6]. Intermediate filling depths cannot be avoided with Floating LNG (FLNG), LNG-Shuttle, and Regasification Vessels (LNG-SRV), because of the production, offloading, and regasification operations.

The simple and obvious solution in the design of an LNG Cargo Containment System (LNG CCS) for all filling operations is to increase the tank structure capacity or to mitigate sloshing pressures. For the LNG-SRV, both wave height and heading are restricted during partial filling operations. In recent FLNG projects, such as the SHELL Prelude FLNG, two-row tank arrangements were adopted to reduce the LNG tank breath, which could mitigate sloshing pressures around 0.30 H fillings.

Several studies aimed to reduce sloshing loads by installing special devices inside the LNG tanks [7, 8]. The construction of these internal devices is costly, and their safety needs to be closely investigated for practical use. It is therefore difficult to make a case for practical application of these slosh reduction devices.

The main objective of the present study was to develop an efficient way to reduce sloshing loads and to investigate a practical method that enables all filling operations. LNG tank shape was tried to be optimized and several candidates of modified LNG tank shape are suggested. Numerical sloshing analysis was carried out to check whether the proposed tanks showed positive results. The numerical sloshing analysis program based on SOLA-VOF, SHI-SLOSH [9, 10], was used for this numerical simulation.

To assess the possibility of practical application, the developed tank shape was also applied to a 160 K LNG carrier. To validate the effectiveness of the optimized

✉ Yonghwan Kim
yhwankim@snu.ac.kr

¹ Marine Research Institute, Samsung Heavy Industries Co., Ltd, Geoje, Gyeongsangnamdo, Korea

² Department of Naval Architecture and Ocean Engineering, Seoul National University, 588 Gwanak-ro, Gwanak-gu, Seoul 151-744, Korea

sloshing reduction design, a series of sloshing model tests were carried out at Seoul National University (SNU). For these tests, 1/50 scaled three-dimensional tanks were manufactured for both the conventional and the modified design. For each tank, 24 types of irregular sea simulations were carried out and dynamic pressures on the tank wall were measured. The measured pressure data were post-processed, and the pressures of two different tanks were statistically compared in several ways.

2 Optimization of LNG tank shape

2.1 Tank shape optimization for all filling operations

Conventional LNG vessels with membrane cargo containment systems have tank filling restrictions based on tank heights [11]. Figure 1 shows typical barred filling range and sloshing impact load of conventional LNG tank. As shown in the red line in the figure, sloshing impact loads are very high in partial filling depth conditions especially around 0.30 H height [1, 2, 5, 6]. To enable unrestricted tank filling operations, it is necessary to reduce sloshing pressures around 0.30 H fillings, or to increase the structural capacity of the LNG CCS.

This study aims to mitigate sloshing pressures by LNG tank shape optimization. To optimize tank shape, a series of numerical sloshing analyses were carried out for various tank shapes. The 160 K LNGC was considered as the reference ship. The dimensions of the conventional tank and several of the optimized tanks are described in Table 1. A computer program developed by Samsung Heavy Industry, SHI-SLOSH, proposed three candidates of the modified tank by increasing the lower chamfer length (Fig. 2; Table 1). The other dimensions were held constant. The total volumes of the considered tanks were therefore smaller than that of the conventional tank. The SHI-SLOSH program was used for the numerical sloshing analysis.

2.2 Numerical method

The flow inside the LNG tank was assumed to be three dimensional, unsteady, incompressible, and viscous. The governing flow equations were the Continuity and Navier–Stokes equations:

$$\nabla \cdot \vec{V} = 0 \tag{1}$$

$$\frac{D\vec{V}}{Dt} = -\frac{1}{\rho} \nabla p + \frac{\vec{f}}{\rho} + \nu \nabla^2 \vec{V}, \tag{2}$$

where \vec{V} is the fluid velocity inside the tank, ρ the fluid density, and ν the kinematic viscosity. \vec{f} is the body force, which could represent the tank motions in six degrees of freedom.

The first-order time marching scheme and central differencing were used for the time and diffusion terms, respectively. Convection terms were discretized with the upwind scheme to increase the method’s numerical stability. The pressure–velocity iteration and free surface movement were solved using the SOLA-VOF method [12]. Dynamic and kinematic boundary conditions were satisfied on the free surface. Due to the limited length of the paper, the details are not described here, but the numerical scheme and validation results were introduced by Park et al. [9, 10].

2.3 Numerical study on tank shape optimization

Numerical computation was carried out for different filling conditions, but the observation on impact loads was focused in 0.30 H filling depth with the beam sea condition, which is a critical filling for LNG cargo design. The speed for the LNGC was assumed to be 5.0 knots at the largest wave heights. The significant wave height (H_s) and zero-crossing periods (T_z) were 12.0 m and 11.0 s, respectively. This condition was 1-year return period of the North Atlantic IACS No. 34. For the beam sea condition, the American Bureau of Shipping [1] and the Lloyd’s Register [2] recommended 1 year, rather than 40-year return

Fig. 1 Typical barred filling range of conventional LNG carriers

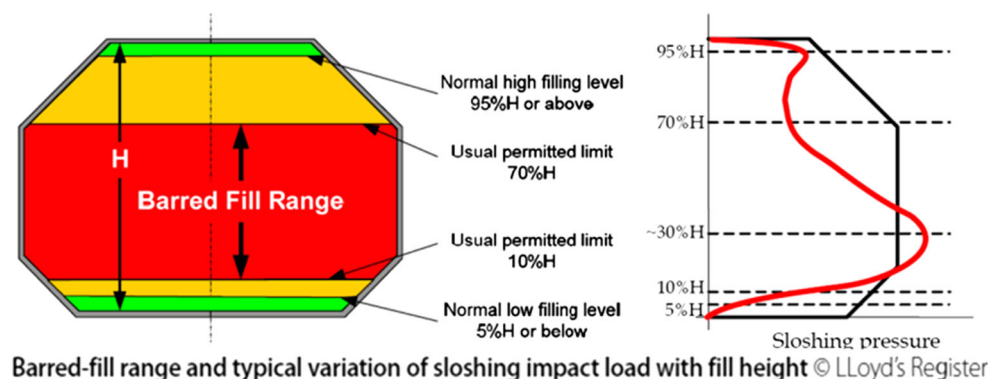
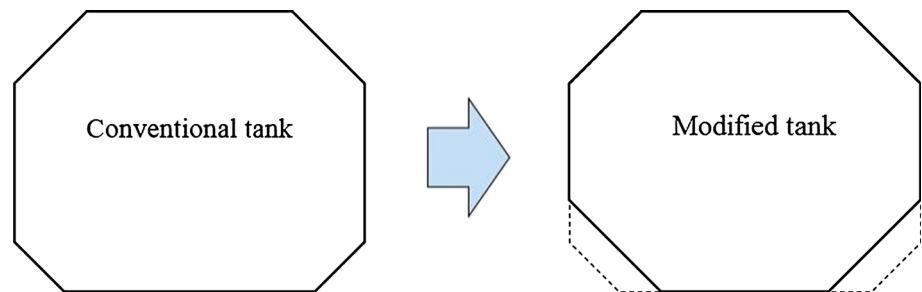


Table 1 Dimensions of the conventional 160 K LNGC and proposed modified tanks

Ship type	160 K LNGC	Tank type 1	Tank type 2	Tank type 3
Tank no.	No. 2 tank	No. 2 tank	No. 2 tank	No. 2 tank
Tank length (m)	46.6	46.6	46.6	46.6
Tank breadth (m)	38.1	38.1	38.1	38.1
Tank height (m)	28.6	28.6	28.6	28.6
Upper chamfer (m)	8.6	8.6	8.6	8.6
Lower chamfer (m)	3.9	6.0	8.0	10.0

Fig. 2 Modified tank shape selection with changing lower chamfer length (*left* conventional tank, *right* modified tank)

periods. The irregular time series of the ship motions in the sloshing calculations was generated by ship RAO (Response Amplitude Operator) and the Bretschneider wave spectrum [10, 13].

All grid space and time steps of these calculations were held constant for all cases to reduce the grid and time dependencies of the present comparative studies. The grid sizes for x , y , and z directions were approximately one meter. The computational time step was 0.0045 s, and the time window was 800 s for all simulations.

The measured sloshing peaks during the numerical simulations of various tanks are presented in Fig. 3a–c and values are in full scale. These are impact pressures on all the side of tank wall, not the time history of any specific point. The sloshing pressures were not much reduced with a small lower chamfer increase, such as Tank Type 1 (Fig. 3b). Tank Type 1 was therefore not appropriate as new design, because the main objective of this study was to reduce sloshing pressures to more below half the pressures of a conventional tank. Sloshing pressures of Tank Type 2 were reduced by more than 50 % compared to the conventional tank (Fig. 3c). A too high chamfer length, such as Tank Type 3 (Fig. 3d), was not practical because the tank volume was reduced too much, and sloshing reduction effect is not that significant compared to Tank Type 2. Also, the too much increase of the lower chamfer height is not practical in ship design.

2.4 Practical tank application for a LNG carrier

The increased lower chamfer length of the selected Tank Type 2 reduced its tank volume compared to the conventional tank (Fig. 2). To practically apply this selected

modified tank type, it was necessary to increase its tank volume to the volume of conventional tank. Tank volume could be increased in several ways, such as by increasing tank breadth, length, or height. Increasing tank breadth and length could result in unexpected high sloshing pressures and it would change the main dimensions of the ship.

Tank height was therefore increased to minimize ship dimension changes. Table 2 shows the final dimensions of optimized tank. The tank's side wall was increased about 1.7 m to maintain the same tank volume as the conventional tank. Other dimensions, such as the beam, length, and upper chamfer of the conventional and modified tank, were held constant. General arrangements of the 160 K LNGC with the conventional and the developed modified tank are shown in Fig. 4. The modified design had no difficulty when applied to the conventional hull shapes.

3 Sloshing model test and validation

3.1 Model test setup

The sloshing model test was carried out to validate the possibility of all filling operations for the developed tank design. The model test was carried out at SNU. A schematic diagram of the sloshing experiment's measurement system is shown in Fig. 5. A motion platform generated the ship motions with six degrees of freedom. Pressure sensors were installed in the tank and measured the dynamic pressure on the tank wall. A data acquisition system converted the electric pressure signal into digital data.

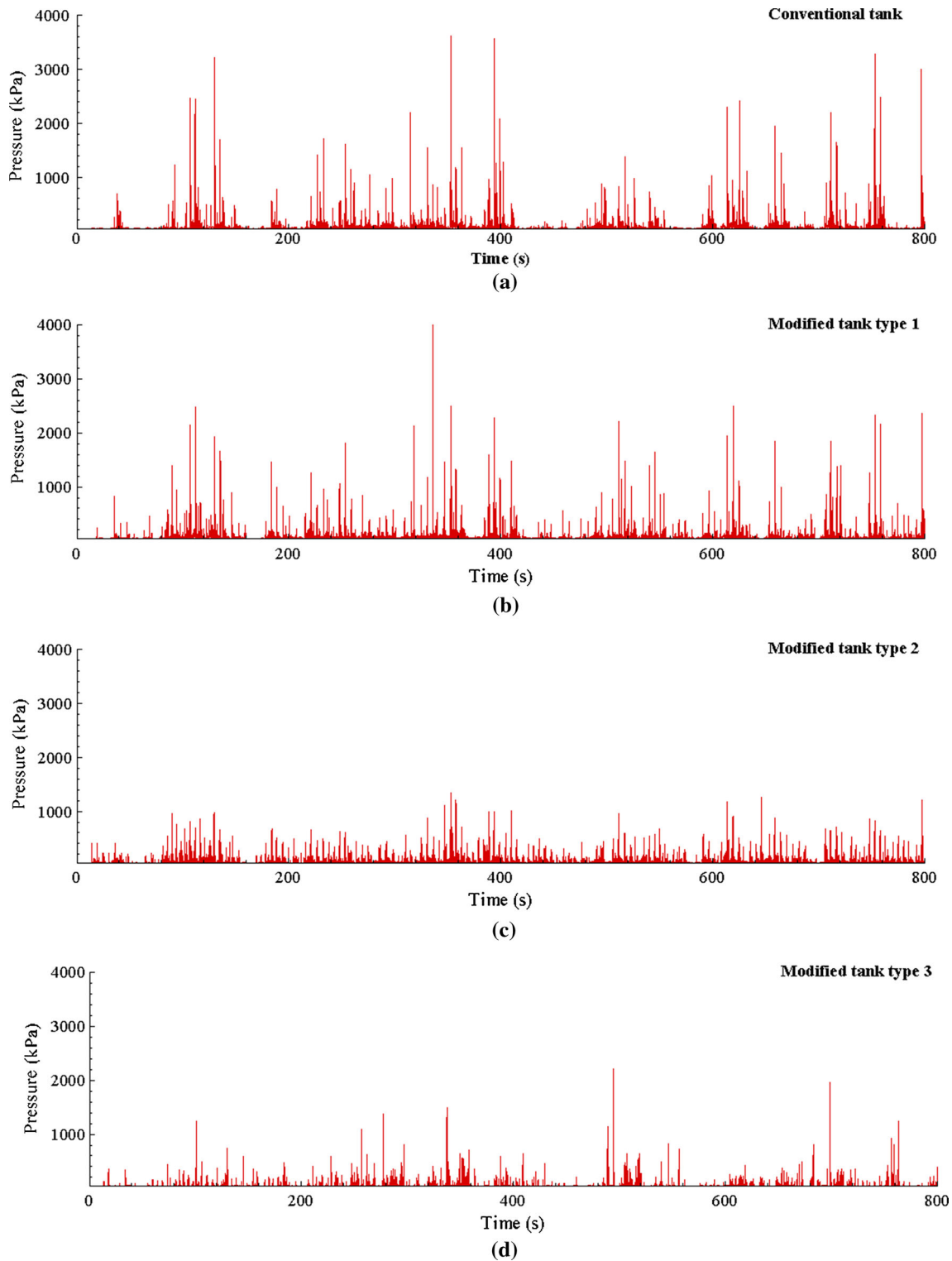


Fig. 3 Sloshing peaks during numerical simulation, full scale (with a 0.30 H filling depth and beam sea condition: $H_s = 12.0$ m, $T_z = 11.5$ s). **a** Conventional LNG tank. **b** Modified tank type 1. **c** Modified tank type 2. **d** Modified tank type 3

Both conventional and modified type 1/50 scaled 160 K LNGC tanks (Figs. 6, 7, respectively) were manufactured for the model tests. Both tanks were made of flexi glass,

and pressure sensors were installed on the tanks using brass sockets. Integrated circuit piezoelectric (ICP) sensors were used to measure dynamic pressures on the tank. Those

Table 2 Comparison of conventional and modified tank dimensions

Ship type	160 K LNGC	Modified tank
Tank length (m)	46.6	46.6
Tank breadth (m)	38.1	38.1
Tank height (m)	28.6	30.3
Upper chamfer (m)	8.6	8.6
Lower chamfer (m)	3.9	8.6

sensors had a 5.54-mm sensing diameter and were installed as cluster at intervals of 10 mm. They were concentrated around three corners and side walls of tank, at the points where high sloshing pressures were expected under the low filling depth condition.

The detailed pressure measuring points of the two tanks are shown in Fig. 8. The measuring points were not exactly the same because the two tanks had different shapes. However, general hot spots were commonly covered for both tanks. For practical reasons, the model tests were carried out using ambient air and water. For more realistic experimental results, it is recommended to match the density ratio of NG and LNG using heavy gas rather than

ambient air. However, the main objective of the present study was to check the effectiveness of the optimized tank. Because the same liquid and gas were used for both the conventional and the modified tank, the influence of the density ratio was not relevant. There are several studies on the influence of liquid–gas density ratio in sloshing [14, 15].

The test conditions are summarized in Table 3. Model tests were carried out at near critical filling depths (0.20–0.40 H). For each filling depth, two wave heading conditions and four wave periods were considered. Therefore, 24 irregular sea ways were simulated for each tank and a total of 48 model test cases were conducted. More intensive sloshing model test cases, such as more filling depths, heading angles, sea states, and repeated tests, will be considered in the future to validate the practical application.

3.2 Analysis of measurement data

The pressure signals of the two different tanks were post-processed statistically to examine the effectiveness of the modified tank as a sloshing reduction device. The peak pressure signals needed to be sampled for the whole

Fig. 4 General arrangement of the 160 K LNG carriers (*top* conventional tank shape, *bottom* developed modified tank)

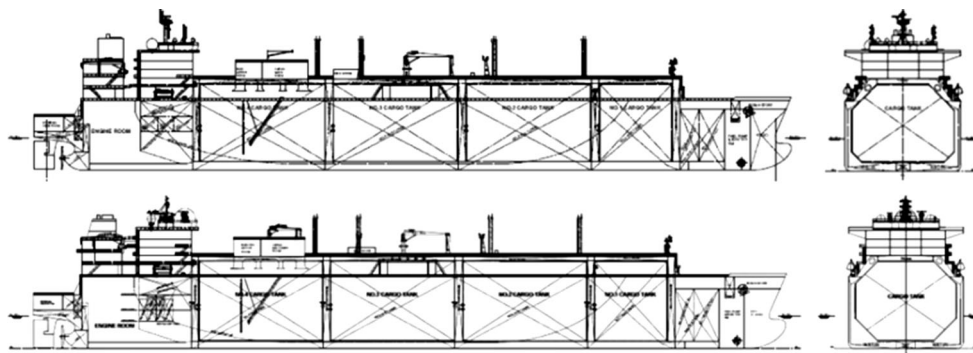
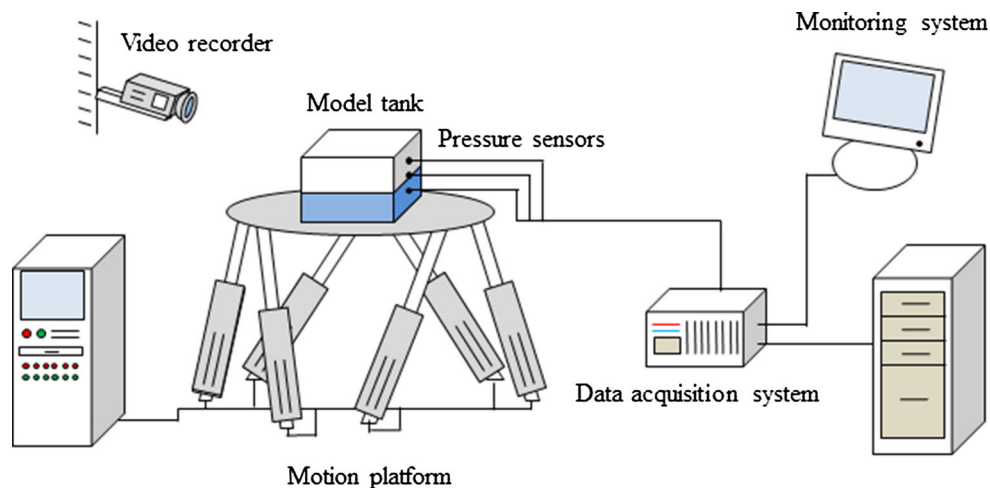


Fig. 5 Schematic diagram of the sloshing experiment's measurement system



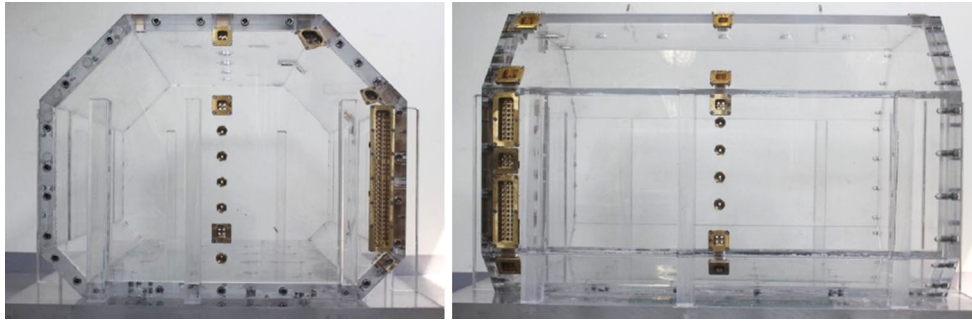


Fig. 6 Conventional tank model for the 160 K LNGC (1/50 scale)

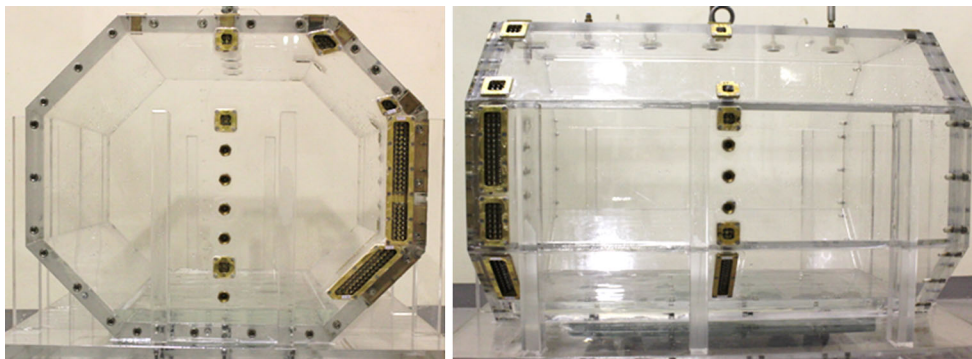


Fig. 7 Modified tank model for the 160 K LNGC (1/50 scale)

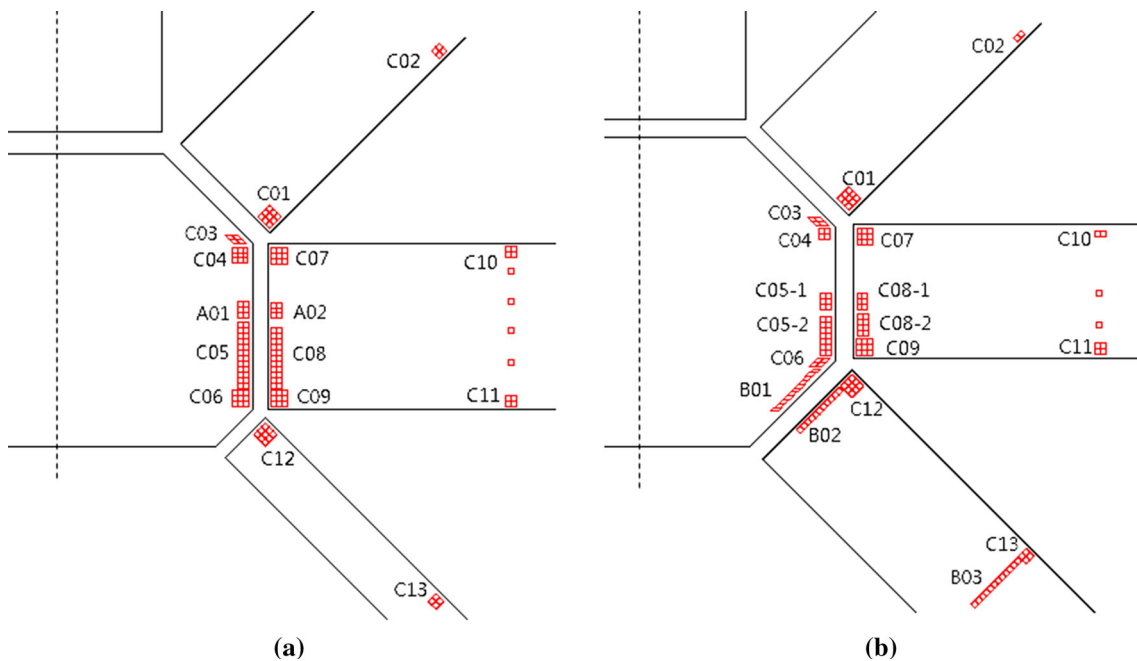


Fig. 8 Locations of pressure sensors in model tests. **a** Conventional tank. **b** Modified tank

pressure time histories. Sampled sloshing peaks, or global peaks, were chosen by imposing a pressure threshold and sampling time window (Fig. 9). Within a moving time

window, the largest peak signal was sampled as the global peak and others were disregarded in the analysis. The maximum pressures collected from all the segments

Table 3 Sloshing experiment conditions of conventional and modified tank

Tank type	No. 2 tank of 160 K LNGC (both conventional and modified tank)
Wave heading	Quartering (150°) and beam (90°) sea
Sea states (North Atlantic no. 34)	40-year return periods for quartering sea condition 1-year return period for beam sea condition
Wave periods	7.5, 9.5, 11.5, 13.5 s
Filling depth	0.20, 0.30, 0.40 H
Ship speed	5 knots
Test time	5 h in full scale

became a set of sampled peaks in the statistical analysis. Peak pressures were defined as the maximum pressure value from each global peak signal. In present study, threshold pressure and sampling time window are fixed as 2.5 kPa and 0.2 s, respectively.

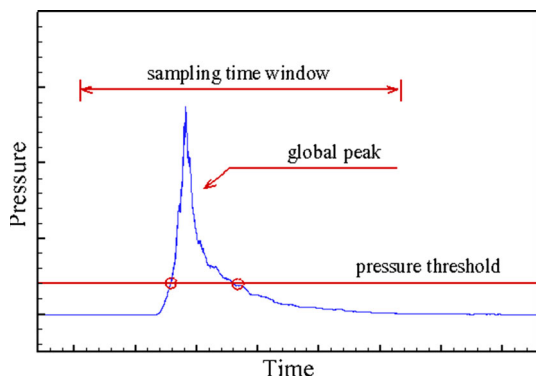
To compare the sloshing severity of the two different tanks, probable extreme pressures were estimated by extreme distribution function fitting. The three-parameter Weibull function was used to represent the probable distribution function of the peak pressures. The cumulative distribution function of the three-parameter Weibull distribution could be written as

$$F(x) = 1 - \exp(-[(x - \delta)/\beta]^\gamma), \quad (3)$$

where δ is the location parameter, β the scale parameter, and γ the shape parameter. Here, x should be larger than the location parameter δ . The method of moments was applied to estimate these three parameters; the first three model moments, mean (μ), variance (σ^2), and skewness (γ_1) were matched with the corresponding sample moments [16].

3.3 Comparison of test results

Sloshing model tests were conducted for various filling and wave conditions for both the conventional and modified tanks, and measured sloshing pressures were compared.

**Fig. 9** Peaks over threshold method

Examples of snap shots for the 0.30 H filling, beam sea case are shown in Fig. 10. It was not easy to define the sloshing load severity by comparing the recorded movies or snap shots. It was observed that when the internal flow approached the corner of the lower chamfer, the conventional tank case showed a very strong impact. For the modified tank, however, the impact was relatively mild and it appeared as major flows climbed up the side wall. This meant that a difference in tank shape possibly changed the sloshing impact hotspots. Movement of sloshing hotspots was therefore also investigated when comparing the pressures on the two tanks.

Examples of pressure time history from two different tanks are shown in Fig. 11. Test condition is 0.20 H filling in beam sea, and pressures are measured at the lower corner of tank side wall which is located at C09 in Fig. 8. Pressure peaks showed irregular trend in both tanks, and large sloshing peaks were occurred at different times in the two tanks. Generally, it appeared as the modified tank reduces sloshing pressure. For more quantitative inspection, statistical pressures needed to be compared.

Figure 12 shows the sloshing pressures of the conventional tank test and given values are scaled to real size. Both the quartering and the beam sea results are shown with changing wave periods. The magnitude of the bar indicates the probable extreme pressure for a 3 h return period. The sloshing peaks were sampled from all sensors installed on the tank. Results of three different fillings were plotted in one graph. The dotted line is an example of the structural dynamic capacity of the membrane LNG CCS on a 0.1-m² panel with utilization factor 0.7 [2, 17]. The capacities of the membrane LNG CCS could be changed depending on the CCS type.

Generally, the conventional tank caused very large sloshing loads in the 0.20 and 0.30 H filling depths (Fig. 12). This is why classification societies placed tank filling restriction on LNG carriers. For the 0.30 H filling, beam sea condition in particular, every four wave periods showed high pressures that exceeded the LNG CCS capacity. To enable partial filling for this conventional tank, it was necessary to increase the LNG CCS capacity by more than two times, which was not practical.

Exceedance probability plots for the sloshing pressure peak measured by all the sensors are shown in Fig. 13. The symbols indicate measured data, and lines represent a fitted Weibull distribution function. Probabilities of the conventional tank tests are more weighted toward the right than those of the modified tank tests. This means that, in the same probability level, modified tank expect lower extreme pressure than conventional tank. The difference of pressures between the two tanks becomes larger after the probability exceeds 10⁻². From this comparison, it could be shown that modified tank is

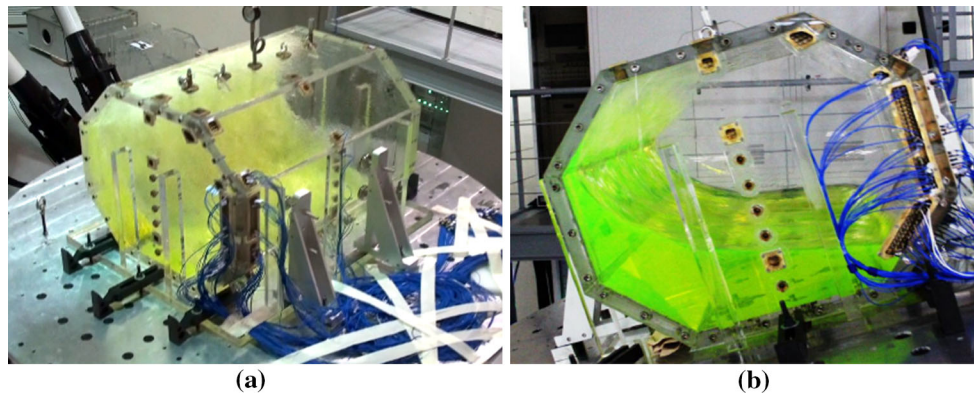


Fig. 10 Free surface movement of model test for 0.30 H filling depth with the beam sea condition: Modified tank. **a** Perspective view. **b** Frontal view

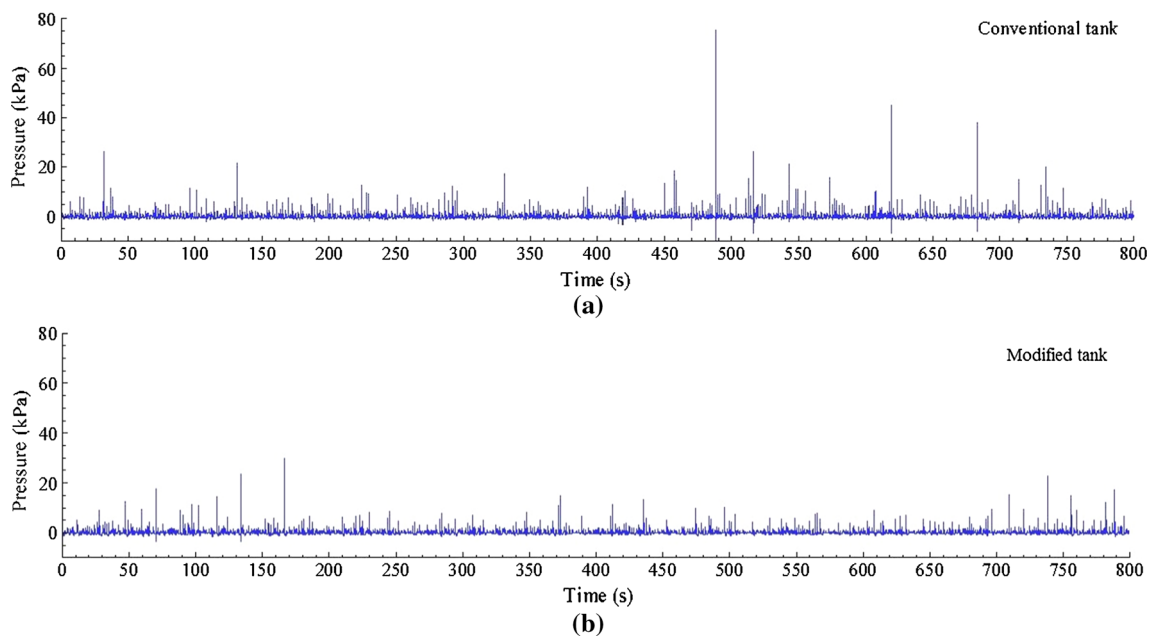


Fig. 11 Time histories of dynamic pressures measured at the lower corner of tank side wall, C09, with a 0.20 H filling depth and beam sea condition, $T_z = 7.5$ s. **a** Conventional tank. **b** Modified tank

effective to mitigate several rarely occurring large sloshing peaks.

Sloshing pressures from the two different tanks were compared (Figs. 14, 15, 16). The 3 h maximum pressures of the conventional and modified tank test are expressed as black and white columns, respectively. Pressures from the 0.40 H filling depth conditions are shown in Fig. 14. In these conditions, the modified tank pressure was not much reduced and some cases showed a slightly increased pressure compared to the conventional tank.

For the 0.30 H filling depth condition, the sloshing pressures of the developed modified tank were, however, much lower than those of the conventional tank (Fig. 15).

Especially for the 0.30 H filling with the beam sea condition, the modified tank reduced sloshing loads to nearly half that of the conventional tank and all the pressures were below the capacity limitation.

Tank shape change also changed the critical heading angle. In the 0.20 H fillings, the conventional tank showed the largest pressures at the quartering sea condition and some cases exceeded the load capacity (Fig. 16). In the modified tanks, the beam sea was, however, much more critical than the quartering sea. Those pressures were, however, also small compared to the conventional tank pressures. Therefore, all modified tank pressures were therefore below the LNG CCS capacity.

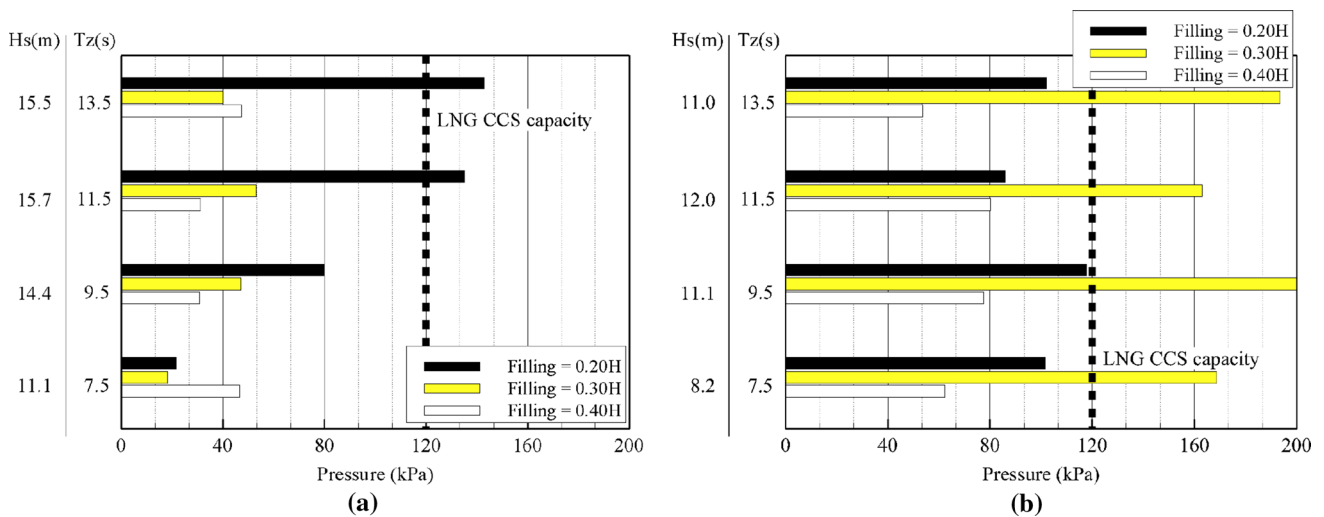


Fig. 12 Sloshing pressures on the conventional tank with various filling depths. **a** Heading angle = 150°, **b** heading angle = 90°

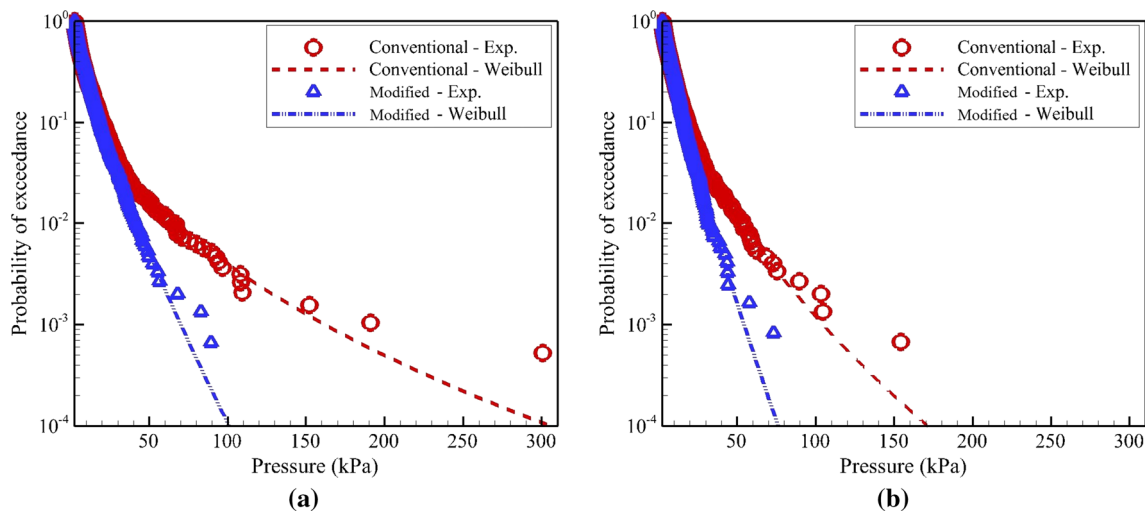


Fig. 13 Comparison of exceedance probability distribution of sloshing peaks between the conventional tank and modified tank, with a beam sea, $T_z = 7.5$ s. **a** Filling depth = 0.30 H. **b** Filling depth = 0.20 H

It is known that beam sea condition is more critical in low filling depth condition. However, due to the highly nonlinear and stochastic character of sloshing phenomenon, exceptional circumstance can arise occasionally (Fig. 16a). Critical heading angle is closely related with water filling depth, tank shape, and wave condition. In an extremely low filling condition, wave breaks very much and fluid is not easy to focus to make large impact. In that case, quartering sea condition concentrate wave to the corner of the tank which has short lower chamfer height (similar height with water filling depth). Those circumstances make it possible to generate high sloshing impact at quartering sea condition rather than beam sea condition in 0.20 H filled conventional tank.

Until now, sloshing severity of the two tank tests was defined based on the measured sloshing peaks sampled from all pressure sensors. It was difficult to compare the sloshing pressures on a specific location. Therefore, extreme pressures from each cluster panels were compared (Fig. 17). As mentioned above, the pressure measuring points of two tanks were not exactly the same. Common hot spots were, however, generally covered and named as ‘Cxx.’ In the 0.40 H filling (Fig. 17a), no panel showed significantly increased sloshing pressures. Increasing the lower chamfer length made C12 and C13 close to the water filling depth, and those two panels showed larger pressure values in the modified tank rather than in the conventional tank. In the 0.30 H filling, C08, which was located on the lower part of the side wall, showed significantly larger

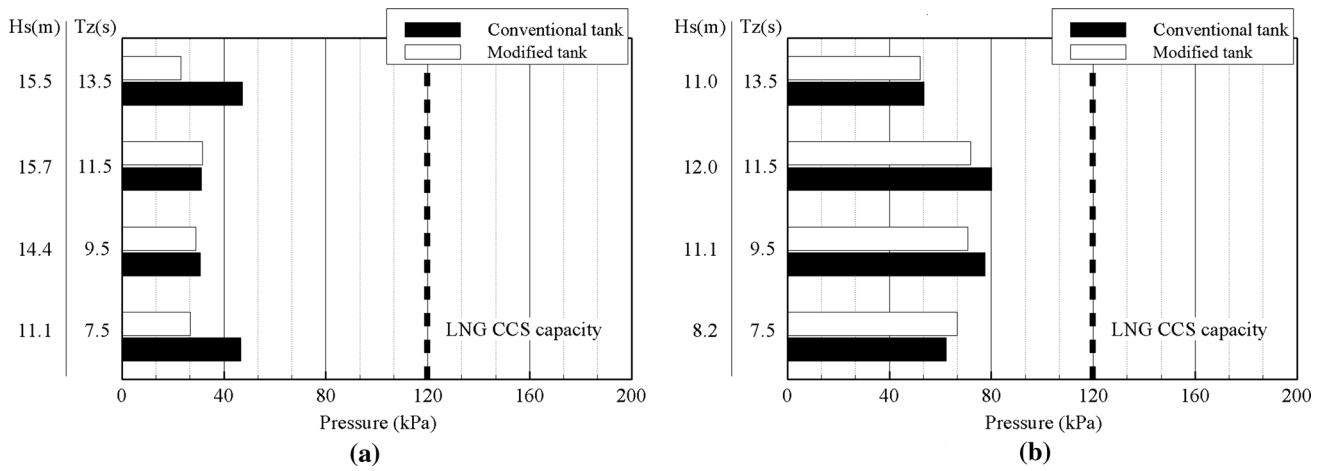


Fig. 14 Comparison of sloshing pressures between the conventional tank and modified tanks: 0.40 H filling depth. **a** Heading angle = 150°. **b** Heading angle = 90°

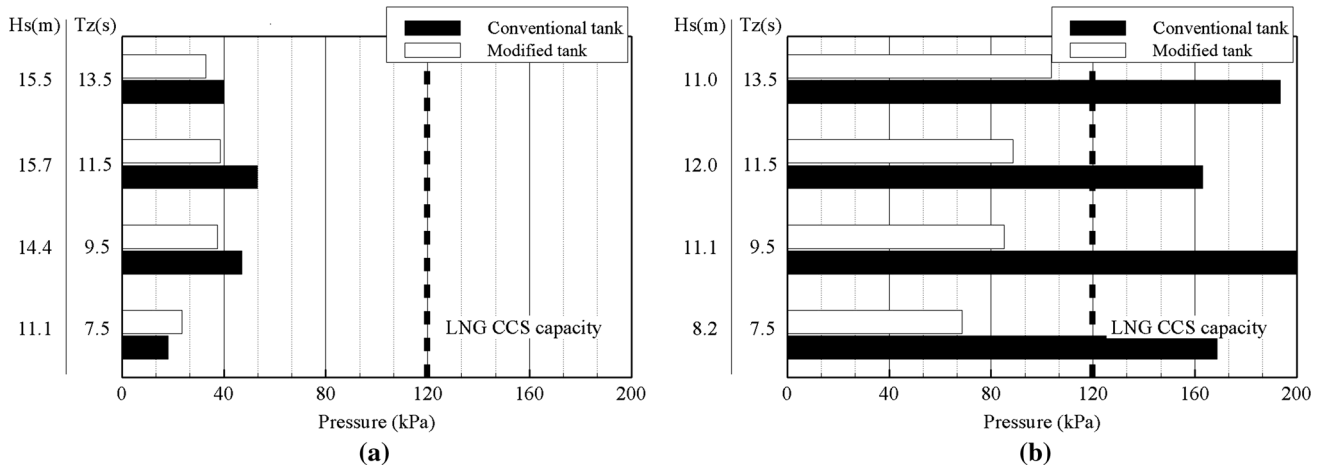


Fig. 15 Comparison of sloshing pressures between the conventional and modified tanks: 0.30 H filling depth. **a** Heading angle = 150°. **b** Heading angle = 90°

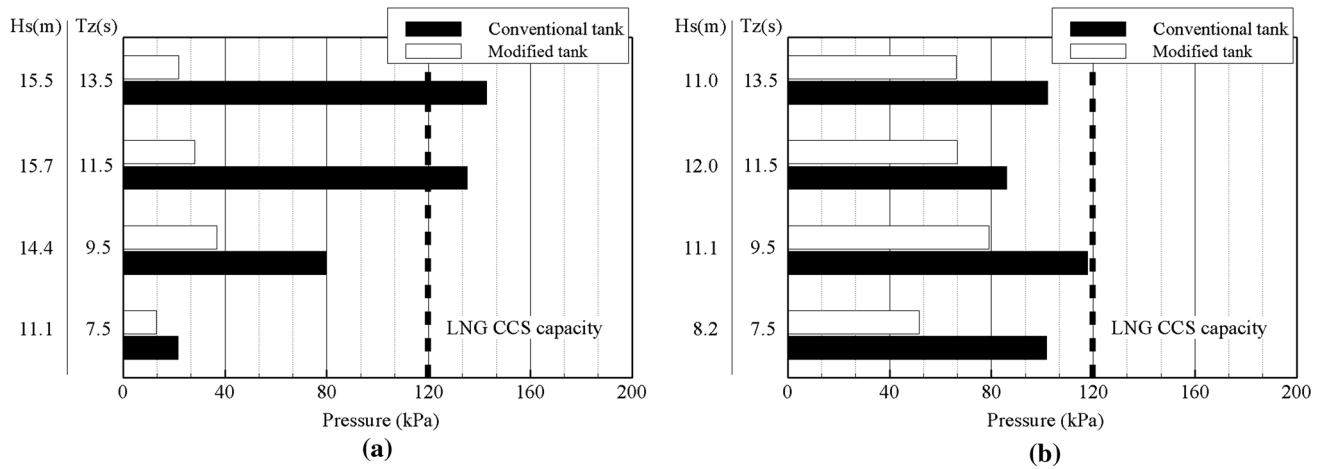


Fig. 16 Comparison of sloshing pressures between the conventional tank and modified tanks: 0.20 H filling depth. **a** Heading angle = 150°. **b** Heading angle = 90°

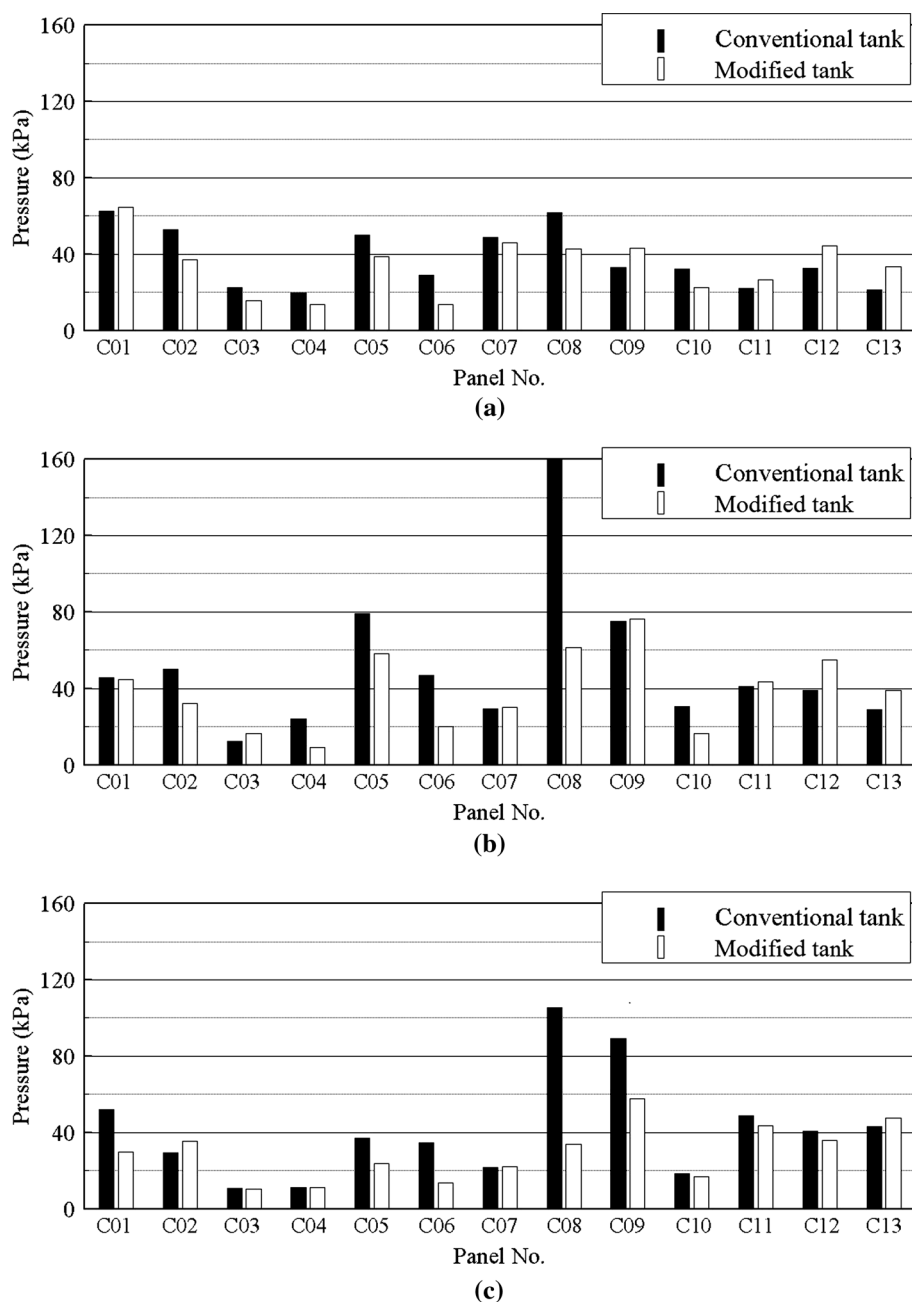
sloshing pressures compared to the other cluster panels. For the modified tank case, however, pressures on C08 reduced dramatically and showed a similar sloshing severity to adjacent panels, such as C05 and C09.

It was obvious that for critical filling depths, the modified tank reduced sloshing pressures on common hotspots. It was a concern whether the modified tank changed the hotspots for sloshing impact and would cause increased sloshing pressures on unexpected regions. Also, in the modified tank, the internal flows showed a tendency to climb up the side wall and a relatively large amount of water reached the upper chamfer region compared to the

conventional tank. Regarding the wave conditions considered in this study, modified type did not significantly increase sloshing loads near the upper chamfer region (C01–C04, C07, C10). This was advantageous for the proposed modified tank.

When considering all results together, the present study showed a possibility of the SHI-designed modified tank as an LNG CCS for all filling operations. For practical application, more detailed sloshing assessments of the modified tank shapes should be carried out, with more test cases, changing panel sizes, and repeated model tests following Class procedures [1, 2].

Fig. 17 Comparison of sloshing pressures on each cluster. **a** Filling depth = 0.40 H, beam sea, $T_z = 9.5$ s. **b** Filling depth = 0.30 H, beam sea, $T_z = 9.5$ s. **c** Filling depth = 0.20 H, beam sea, $T_z = 9.5$ s



4 Conclusions

The present study suggested an efficient way to reduce sloshing pressures on a conventional LNG cargo tank by tank shape optimization. Numerical sloshing analysis was carried out to find the modified tank design that is appropriate for all filling operations. After tank design optimization, 1/50 scale sloshing model tests were carried out for validation purposes. The following conclusions could be made:

- Conventional LNGC tank design, which has a small lower chamfer, was not applicable for all filling operation. In a 1/50 scale conventional tank, very large sloshing pressures were measured at 0.30 H filling, beam sea conditions. In these conditions, any zero-crossing wave period from 7.5 to 13.5 s could be critical to the tank structure.
- Several optimized tank models were suggested by increasing lower chamfer length. Based on numerical results, it was found that sloshing load was sensitive to lower chamfer size. For sloshing reduction, a lower chamfer length of about 30 % tank height was suggested.
- Effectiveness of optimized tank design was validated not only in numerical calculation but also in experimental analysis. In the 1/50 scale model tests, extreme sloshing pressures of the modified tank were less than half those of the conventional tank in critical filling depth condition.
- There was a slight change in sloshing hotspots in the modified tank. Pressures on the lower chamfer were increased, but this was not critical for CCS design. Regardless, the 0.30 H filling showed relatively large sloshing pressures compared to the other filling depth condition. Also, the modified design did not significantly increase sloshing loads on unexpected regions, for example, the corner of the upper chamfer.
- In summary, the developed modified tank shape provided a possibility for all filling operations of the 160 K LNG CCS.

References

1. American Bureau of Shipping (2009) Guidance Notes on Strength Assessment of Membrane-Type LNG Containment Systems under Sloshing Loads. Guidance note, Houston, USA
2. Lloyd's Register (2009) Sloshing Assessment Guidance Document for Membrane Tank LNG Operations. Guidance note, London, UK
3. Lee H, Kim JW, Hwang C (2004) Study on coupling effects of ship motion and sloshing. *J Ocean Eng* 34:2176–2187
4. Macdonald AJ (2008) Lloyd's Register's guidance on the operation of membrane LNG ships to avoid the risk of sloshing damage. In: Proceedings of GASTECH, Bangkok, Thailand
5. Pastoor W, Tveitnes T, Valsgard S, Sele HO (2004) Sloshing in partially filled LNG tanks: an experimental survey. In: Proceedings of the 5th offshore technology conference, OTC, Houston, USA
6. Zhao R, Rognebakke O, Zheng X (2004) Wave and Impact Loads in Design of Large and Conventional LNG Ships. In: Proceedings of RINA conference of design and operation of gas carriers, London, UK
7. Anai Y, Ando T, Watanabe N, Murakami C, Tanaka Y (2010) Development of a New Reduction Device of Sloshing Load in Tank. In: Proceedings of the 20th international offshore and polar engineering conference, ISOPE, Beijing, China
8. Kim Y, Kim SY, Ahn Y, Kim KH, Jeon SE, Shu YS, Park JJ, Hwangbo SM (2013) Model-scale sloshing tests for and anti-sloshing blanket system. *Int J Offshore Polar Eng* 23(4):252–254
9. Ha MK, Kim MS, Paik BK, Park CH (2002) Motion and sloshing analysis for new concept of offshore storage unit. *Int J Ocean Eng Tech* 16(1):1–7
10. Park JJ, Kim MS, Kim YB, Ha MK (2006) Practical Application of Numerical Sloshing Analysis for Development of Large LNG Carriers. In: Proceedings of the 16th international offshore and polar engineering conference, ISOPE San Francisco, USA
11. Lloyd's Register (2012) Guidance on the Operation of Membrane LNG Ships to Reduce the Risk of Damage due to Sloshing, Guidance note, London, UK
12. Nichols BD, Hirt CW (1971) Improved free surface boundary conditions for numerical incompressible-flow calculations. *J Comp Phys* 8:434–448
13. Lloyd ARJM (1989) Seakeeping : Ship behavior in rough weather. Ellis Horwood Ltd, UK
14. Maillard S, Brosset L (2009) Influence of Density Ratio between Liquid and Gas on Sloshing Model Test Results In: Proceedings of the 19th international offshore and polar engineering conference, ISOPE, Osaka, Japan
15. Ahn Y, Kim SY, Kim KH, Lee SW, Kim Y, Park JJ (2012) Study on the Effect of density Ratio of Liquid and Gas in Sloshing Experiment. In: Proceedings of the 22nd international offshore and polar engineering conference, ISOPE, Rhodes, Greece
16. Kim, SY, Kim Y, Kim, KH (2013) Statistical Analysis of Sloshing-Induced Random Impact Pressures. *J Eng Mari Env* [Online] Available: <http://pim.sagepub.com>
17. Chun SE, Hwang JO, Chun MS, Lee JM, Suh YS, Hwangbo, SM (2011) Direct Assessment of Structural Capacity against Sloshing Loads using Nonlinear Dynamic FE analysis including Hull Structural Interactions. In: Proceedings of the 21st international offshore and polar engineering conference, ISOPE, Hawaii, USA